by treatment with EGF (300 ng/ml, 10 min). Immunoprecipitated [^{32}P]PLC-γ1 was incubated with phosphatases for 90 min under conditions used for the experiments shown in Fig. 3A. PLC-γ1 was separated by SDS-PAGE and labeled proteins were transferred to Immobilon P. After visualization by autoradiography, phosphoamino acid analysis was performed on the bands that corresponded to PLC-γ1.
18. D. E. Cool *et al.*, *Proc. Natl. Acad. Sci. U.S.A.* **86**, 5257 (1989).
19. S. Nishibe and G. Carpenter, unpublished data.
20. N. K. Tonks, H. Charbonneau, C. D. Diltz, E. H. Fischer, K. A. Walsh, *Biochemistry* **27**, 8695 (1988).
21. S. M. T. Hernández-Sotomayor, S. Nishibe, G. Carpenter, unpublished data.
22. N. G. Anderson, J. L. Maller, N. K. Tonks, T. W. Sturgill, *Nature* **343**, 651 (1990).
23. We thank D. Sanchez for technical assistance; S. Heaver for typing the manuscript; J. Maller and M. Mumby for the generous gift of phosphatase 2A; and D. Cool, C. Diltz, J. Lorenzen, and N. Zander for preparation of phosphatase. Supported by NIH grants GMO7347 and CA43720 and American Cancer Society grant RD304.

30 May 1990; accepted 14 August 1990

Kinetics of Gramicidin Channel Formation in Lipid Bilayers: Transmembrane Monomer Association

ANNE M. O'CONNELL, ROGER E. KOEPPE II, OLAF S. ANDERSEN

Conducting gramicidin channels form predominantly by the transmembrane association of monomers, one from each side of a lipid bilayer. In single-channel experiments in planar bilayers the two gramicidin analogs, [Val^1]gramicidin A (gA) and [4,4,4-F$_3$-Val^1]gramicidin A (F$_3$gA), form dimeric channels that are structurally equivalent and have characteristically different conductances. When these gramicidins were added asymmetrically, one to each side of a preformed bilayer, the predominant channel type was the hybrid channel, formed between two chemically dissimilar monomers. These channels formed by the association of monomers residing in each half of the membrane. These results also indicate that the hydrophobic gramicidins are surprisingly membrane impermeant, a conclusion that was confirmed in experiments in which gA was added asymmetrically and symmetrically to preformed bilayers.

GRAMICIDIN CHANNELS ARE MEMbrane-spanning structures that serve as prototypical models for studying mechanisms of ion permeation, lipid-protein interactions, and conformational dynamics of ion-permeable channels (*1*). The primary sequence of gA is (*2*):

Formyl-L-Val–Gly-L-Ala-D-Leu-L-Ala-
D-Val-L-Val-D-Val-L-Trp-D-Leu-L-Trp-
D-Leu-L-Trp-D-Leu-L-Trp-ethanolamine

The mechanism of gramicidin channel insertion into lipid bilayers is poorly understood because the membrane-spanning channels are formyl-NH-to-formyl-NH terminal dimers of β$^{6.3}$-helices, as suggested by Urry (*3*), whereas gramicidins dissolved in organic solvents exist as mixtures of parallel and antiparallel intertwined dimers and disordered monomers (*4*–*6*), depending upon solvent type and gramicidin concentration. Gramicidins therefore undergo conformational changes in their transition from dissolved molecules to molecules dispersed in water (*7*) and finally to membrane-spanning channels. Furthermore, as membrane-associated gramicidins exist in a number of (slowly interconverting) conformational states (*8*), it is not known whether the major pathway for channel formation involves the membrane insertion of (antiparallel) intertwined dimers with a subsequent formation of the β$^{6.3}$-helical dimer (*9*) or the transmembrane association of β-helical monomers residing in opposite monolayers (Fig. 1).

We addressed the channel formation problem by exploiting the following features of gramicidin channels: (i) gramicidin channels are symmetrical dimers (*10*), with a single predominant conductance state (*11*); (ii) sequence-substituted gramicidins form symmetrical channels (or homodimers) that have different conductances (*12*); and (iii) hybrid channels (or heterodimers) form between the chemically dissimilar analogs (*12, 13*). One can thus use the amplitude of individual channel events in a real-time assay to identify which molecules form each conducting event.

In 1.0 M CsCl, the conductances of gA and F$_3$gA channels differ threefold because of the -CF$_3$ substitution in F$_3$gA (*12*). When either gramicidin is added symmetrically to the aqueous solutions on both sides of a bilayer, a single characteristic channel type is observed (Fig. 2, A and B). When both gramicidins are added symmetrically, three channel types are observed (Fig. 2C), corresponding to the two homodimers and the heterodimer (*12*).

When gA and F$_3$gA are added asymmetrically to opposite sides of a preformed bilayer, all three channel types are again observed (Fig. 3, A through C). However, when the channel appearance rates are plotted versus time, the heterodimers dominate throughout all but the first few minutes (Fig. 3D). The homodimer appearance rates remain stable and may decrease slightly during the first few minutes. The dominance of heterodimers shows that under our conditions (6 to 15 pM gramicidin dispersed in water from a 15 nM solution in ethanol) most gramicidin channels result from the transmembrane association of β$^{6.3}$-helical monomers as outlined in Fig. 1A.

After 20 min, the membranes were broken and reformed in order to equilibrate both gramicidins between the monolayers. A large change in the channel appearance pattern occurred (Fig. 3C): the homodimer appearance rates increased, and the heterodimer appearance rate decreased (*15*).

Comparable results were obtained when only gA was added to one side, or to both sides, of preformed bilayers (Fig. 4). In these experiments, the gramicidin concen-

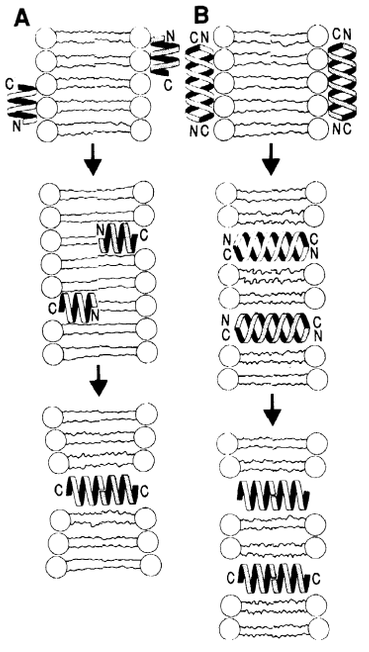

Fig. 1. Schematic representation of two gramicidin channel insertion mechanisms. (**A**) Dimerization of β$^{6.3}$-helical monomers (from each side of the membrane). Gramicidin monomers adsorb to each monolayer from the immediately adjacent aqueous solution and fold into β$^{6.3}$-helices (top), folded monomers insert into each monolayer (middle), and dimerize to form the channel (bottom). (**B**) Insertion of intertwined antiparallel dimers followed by unwinding to form β$^{6.3}$-helical dimers. Intertwined dimers adsorb to each monolayer (top), insert to span the membrane (middle), and unwind to form the channels (bottom).

A. M. O'Connell and O. S. Andersen, Department of Physiology and Biophysics, Cornell University Medical College, New York, NY 10021.
R. E. Koeppe II, Department of Chemistry and Biochemistry, University of Arkansas, Fayetteville, AR 72701.

tration in the one-sided experiments was twice that in the two-sided experiments to ensure that the total amount of gramicidin (in both halves of the bilayer) was the same in both experiments (*16*). After symmetrical addition, the channel appearance rate increased steadily for the duration of the experiment, paralleling the hybrid channel pattern in Fig. 3. After asymmetrical addition, a constant, low channel appearance rate was achieved in the first few minutes of the experiment that was similar to the pattern for the homodimers in Fig. 3. After 17 min, the membranes were again broken and reformed, which resulted in a ~100-fold increase in channel activity in the case of asymmetrical addition, as compared to only a 2-fold increase after symmetrical addition. The final channel activity was similar for both conditions.

These results show that gramicidin molecules permeate poorly across lipid bilayers. Otherwise the transmembrane difference in gA surface densities necessary to account for the difference in channel activity between the symmetrical and asymmetrical additions could not be maintained (*17*).

The early appearance of a few homodimers during the first minutes after gramicidin addition (Fig. 3) suggests that gramicidin channels also can form by an alternative mechanism in which both monomers originate from the same side of the membrane. When dissolved in ethanol, gA forms intertwined dimers (*4, 18*) that could adsorb at the membrane-solution interface (*19*). Homodimers thus might form because such intertwined dimers insert, span the bilayer, and unwind to form $\beta^{6.3}$-helical dimers (Fig. 1B) or because the intertwined dimers unfold at the interface and refold to form $\beta^{6.3}$-helical dimers that insert to span the bilayer. Alternatively, "islands" of high peptide (and solvent) concentration might exist transiently in the membrane after gramicidin addition, resulting in local bilayer disruption and allowing for peptide transfer.

In Fig. 4, the attainment of an apparently constant appearance rate early in the asymmetrical experiments also indicates that a few (early) gramicidin channels form by a mechanism different from that by which the later channels form. This question was investigated further in experiments in which we were able to differentially modulate the formation of channels by monomers originating from each of two or from only one aqueous compartment.

For the experiments in Fig. 5A, the bilayers were modified by 1-monopalmitoylphosphatidylcholine (MPPC), which increases gramicidin channel activity by increasing the equilibrium constant for channel formation (*11*). The results for asymmetrical addition of gA and F_3gA were similar to those in Fig. 3. The heterodimer appearance rate increased steadily throughout the experiment; the homodimer appearance rates remained low and stable. Quantitatively, the heterodimer appearance rate increased ~50% faster than in the absence of MPPC, while the homodimer appearance rates were unaffected. Thus MPPC seems to increase the rate of channel formation by transmembrane dimerization but does not affect the formation of channels by a "cis" mechanism.

For the experiments in Fig. 5B, gA was dissolved in trifluoroethanol, in which it is monomeric (*20*) although not necessarily helical. When gA was added asymmetrically from this solvent, the channel appearance rate was twofold less than when gA was dissolved in ethanol. Thus, the minor cis mechanism for channel formation appears to be affected by the solvent history of the gramicidin.

In any case, since the predominant mechanism for channel formation involves the transmembrane association of monomers, one can from the principle of detailed balance (*21*) deduce that the disappearance of the early homodimers results in the transfer of gramicidin monomers into the trans monolayer. These "transferred" monomers can then associate with monomers in the cis monolayer and produce homodimers (*22*). A "loss" of some of this transferred peptide from the inserted to the trans-adsorbed conformation may account for the slight "burst" of homodimer activity during the first minutes in Fig. 3 and Fig. 4, A to C. The completion of this process after 1 to 2 min sets an upper limit on the molecules' confor-

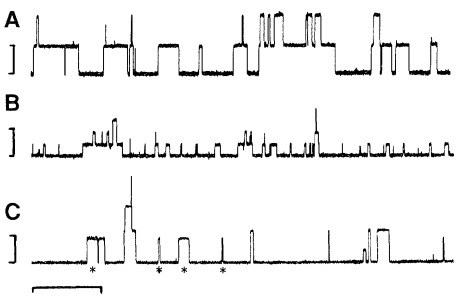

Fig. 2. Single-channel current traces after symmetrical addition of gramicidin to both aqueous solutions bathing a preformed membrane. (**A**) After addition of only gA. All channel appearances have a single characteristic amplitude. (**B**) After addition of only F_3gA. Most channel appearances have a characteristic amplitude that differs from that observed with gA. (The two "aberrant" transitions are heterodimers formed between F_3gA and contaminating gA.) (**C**) After addition of both gA and F_3gA. In addition to the two homodimeric channel types a new channel type is observed that corresponds to the heterodimers (some of these are marked by asterisks). Similar results were obtained in all ($n > 10$) experiments [see also (*12, 13*)]. Single-channel recordings (100 mV, 80 Hz) were made in bilayers across a hole (area ~0.07 mm^2) in a Teflon partition separating two 5-ml Teflon chambers (*14*). The bilayers were formed from 40-mg/ml diphytanoylphosphatidylcholine (DPhPC) in *n*-decane. This solution was used for all experiments except those in Fig. 5A. The aqueous solutions were unbuffered 1.0 M CsCl, and the gramicidins were added as 2- to 10-μl aliquots from ethanolic stock solutions (except for the experiments in Fig. 5B). Calibration bars: horizontal, 10 s; vertical, 1 pA.

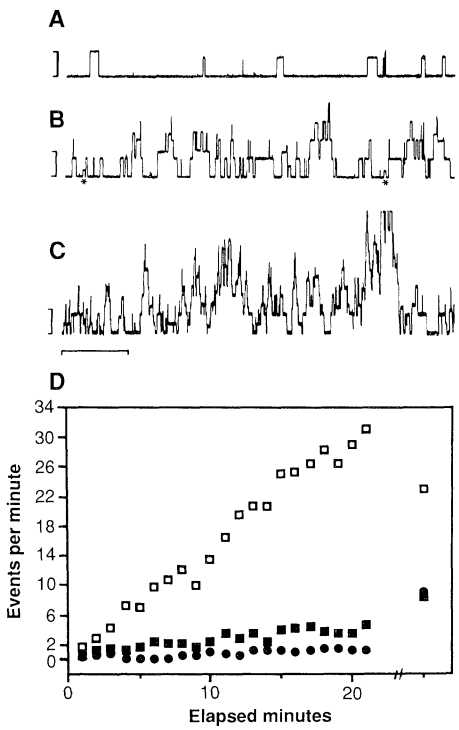

Fig. 3. Current traces from the first (**A**) and twelfth (**B**) minute after one-sided addition of gA to one side and F_3gA to the other side of a preformed membrane, and (**C**) after breaking and reforming the membrane. Asterisks (B) mark homodimeric F_3gA channels. Equipotent amounts of gA and F_3gA were added during vigorous stirring to the opposing aqueous solutions separated by the membrane. Stirring was continued for 30 s, and the potential was applied within 3 s. Other conditions and calibration as in Fig. 2. (**D**) Average number of each channel type observed during each minute after gramicidin addition [gA homodimers (■), F_3gA homodimers (●), and gA-F_3gA heterodimers (□)]. Each point denotes an average of six experiments. Zero time is when the potential is applied. The break in the abscissa denotes when the membranes were broken with a large voltage pulse and reformed (repainted) within 30 s using no additional lipid. The membrane capacitance was monitored throughout each experiment to monitor the membrane area, which varied by less than 10%. At the end of the experiment before breaking the membrane, the ratio $f_h/(2[f_a f_b]^{0.5})$ [where f_h, f_a, and f_b denote the appearance rates of the heterodimers and two homodimers, respectively (*13*)] varied between 5 and 15, and decreased to between 1 and 2 after reforming the bilayer.

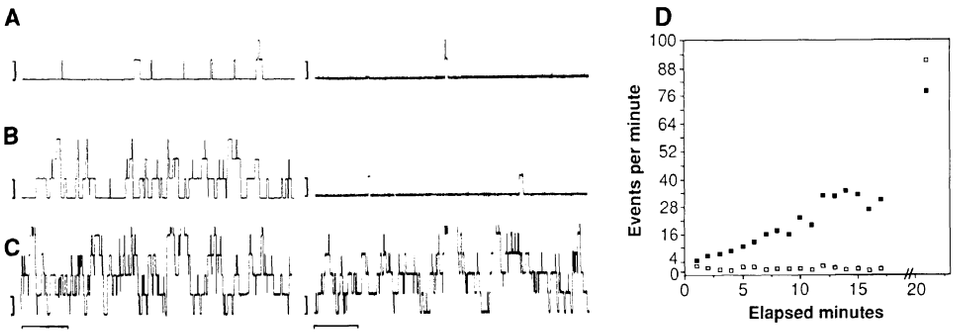

Fig. 4. (**A** through **C**) Current traces after symmetrical (left) and asymmetrical (right) addition of gA, from (A) the first and (B) tenth minute, and (C) after breaking and reforming the membrane. Calibration bars: horizontal, 10 s; vertical, 1 pA. (**D**) Average number of channel events during each minute, and after breaking and reforming the membranes, after adding only gA to one (□, $n = 4$) or both (■, $n = 2$) sides of preformed membranes. The break in the abscissa denotes when the membranes were broken and reformed. In the asymmetrical experiments, there were 0 to 6 channel appearances/min (average of 0.9 appearances per minute). After breaking and reforming the bilayer, the appearance rate increased 50- to 130-fold over the average rate before breaking the membrane (to 35 to 135 appearances per minute). During the course of the symmetrical experiments, there was a 6- to 12-fold increase in channel activity, which increased an additional 2-fold after breaking and reforming the membrane.

mational "memory" of their solvent history after exposure to the aqueous solution and membrane-solution interface (*8, 23*).

In these experiments the channels were standard gramicidin channels and did not resemble the long-lived events that would be expected if they were formed by the intertwined dimers themselves (*24*). However, the gramicidin:lipid ratio in the bilayers was $\sim 10^{-7}$, such that the gramicidins at equilibrium should be predominantly monomeric (*23*). At higher gramicidin:lipid ratios, $\beta^{6.3}$-helical channels might form by the unwinding of membrane-spanning dimers if the intertwined helices had the same handedness as the $\beta^{6.3}$-helical dimers (*25*).

The large difference in channel appearance rates between the asymmetrical and symmetrical gA additions (Fig. 4) shows that lipid bilayers are surprisingly impermeable to gramicidin molecules. This impermeability is a property of the COOH-terminal half of the molecule (because the formyl-NH-terminus inserts into the bilayer en route to forming the $\beta^{6.3}$-helical conducting dimer). The four indole >NH groups could hydrogen bond to water or to the phospholipid backbone and give the COOH-terminal half of the molecule a greater preference for the membrane-solution interface over the interior than would be predicted from hydrophobicity alone (*26*). Consistent with this notion, the channel-forming potency of [Trp^1]gA is 300-fold less than that of gA (*27*), and in the bacterial reaction center tryptophans tend to reside close to the membrane-solution interface (*28*).

The insertion of integral membrane proteins is an unresolved problem in membrane biophysics (*29*). The situation in vivo is more complex than what we have described here. Nevertheless, we note that the gramicidins are extremely hydrophobic yet almost impermeant, which implies that they partition poorly into the membrane interior. This result suggests that amino acids' hydrophobic index (*30*) should be redefined to vary with the position of the residues in the three-dimensional structure of the folded membrane-inserted proteins. We finally note that the resolution allowed by single-channel recordings, where one by definition observes single molecular assemblies, also might be of use to study the insertion and assembly of integral membrane proteins.

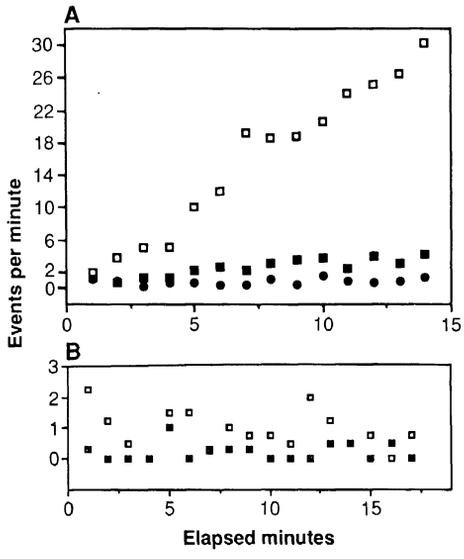

Fig. 5. (**A**) Average number of each channel type during each minute after asymmetrical addition of gA and F_3gA to preformed membranes formed from a 100:1 mixture of DPhPC and MPPC in *n*-decane (40 mg/ml); gA homodimers (■), F_3gA homodimers (●), and gA-F_3gA heterodimers (□). Each point denotes the average of five experiments. At the end of the experiment before breaking the membrane, $f_h/(2[f_a f_b]^{0.5})$ varied between 2 and 15. Because of the presence of MPPC, the channel activity was too high after breaking and reforming the membranes to allow quantification of the channel frequencies. (**B**) Average number of channel events during each minute after asymmetrical addition of gA dissolved in trifluoroethanol (⊠). Each point denotes the average of three experiments. There were 0 to 2 channel appearances per minute (average of 0.2 appearances per minute). After breaking and reforming the bilayer, the appearance rate increased 300- to 800-fold over the average rate before breaking the membrane (to 80 to 130 appearances per minute). For comparison, the results for asymmetrical addition from ethanol are reproduced from Fig. 4D (□).

REFERENCES AND NOTES

1. A. Pullman, J. Jortner, B. Pullman, Eds., *Transport through Membranes: Carriers, Channels and Pumps* (Kluwer Academic, Dordrecht, 1988).
2. R. Sarges and B. Witkop, *J. Am. Chem. Soc.* **87**, 2011 (1965).
3. D. W. Urry, *Proc. Natl. Acad. Sci. U.S.A.* **68**, 672 (1971).
4. W. R. Veatch and E. R. Blout, *Biochemistry* **13**, 5257 (1974).
5. S. V. Sychev *et al.*, *Bioorgan. Chem.* **9**, 121 (1980); G. E. Hawkes, L.-Y. Lian, E. W. Randall, K. D. Sales, E. H. Curzon, *Eur. J. Biochem.* **166**, 437 (1987); V. F. Bystrov and A. S. Arseniev, *Tetrahedron* **44**, 925 (1988); P. E. Easton, thesis, University of Arkansas, Fayetteville (1989); B. Roux, thesis, Harvard University, Cambridge, MA (1990).
6. D. A. Langs, *Science* **241**, 188 (1988); B. A. Wallace and K. Ravikumar, *ibid.*, p. 181.
7. The gramicidins are not soluble in aqueous solutions but seem to aggregate into poorly defined entities [G. Kemp and C. Wenner, *Arch. Biochem. Biophys.* **176**, 547 (1976)].
8. J. A. Killian and D. W. Urry, *Biochemistry* **27**, 7295 (1988); P. V. LoGrasso, F. Moll III, T. A. Cross, *Biophys. J.* **54**, 259 (1988).
9. B. A. Wallace, in *Ion Transport Through Membranes*, K. Yagi and B. Pullman, Eds. (Academic Press, Tokyo, 1987), pp. 255–275; J. A. Killian and B. de Kruijff, *Biophys. J.* **53**, 111 (1988); F. R. Salemme, *Science* **241**, 145 (1988).
10. A. S. Cifu, R. E. Koeppe II, O. S. Andersen, *Biophys. J.* **55**, 503a (1989); see also articles in (*1*).
11. D. B. Sawyer, R. E. Koeppe II, O. S. Andersen, *Biochemistry* **28**, 6571 (1989).
12. E. W. B. Russell, L. B. Weiss, F. I. Navetta, R. E. Koeppe II, O. S. Andersen, *Biophys. J.* **49**, 673 (1986).
13. J. T. Durkin, R. E. Koeppe II, O. S. Andersen, *J. Mol. Biol.* **211**, 221 (1990).
14. O. S. Andersen and R. U. Muller, *J. Gen. Physiol.* **80**, 403 (1982).
15. If both gramicidin analogs were distributed symmetrically (at one half their respective surface densities before the membranes were broken) after breaking and reforming the membranes, the heterodimer appearance rate (f_h) should decrease by one half and be related to the homodimer appearance rates (f_a and f_b, respectively) by the relation $f_h \geq 2(f_a f_b)^{0.5}$ (*13*).
16. The different concentrations were chosen for two reasons. If gramicidin channels predominantly form by the unwinding of membrane-spanning intertwined dimers, the channel appearance rate should be the same for the asymmetrical and symmetrical experiments. Also, if the membrane permeability of gA was much higher than its aqueous convergence permeability, the interfacial gA concentration (and thus the channel activity) should be the same for the symmetrical and asymmetrical experiments (and the gA distribution should be the same before and after breaking and reforming the membranes).
17. Because the channels are dimers, one might expect that the channel appearance rate in the symmetrical

experiments should increase proportionate to t^2, where t is the time after gramicidin addition [S. B. Hladky, in *Drugs and Transport Processes*, B. A. Callingham, Ed. (Macmillan, London, 1974), pp. 193–210]. This effect is observed, however, only if the surface density of $\beta^{6.3}$-helical monomers increases as a linear function of t. The approximately linear increase in channel activity over time results because gramicidin channels form by several parallel sequential processes. See also D. C. Buster, J. F. Hinton, F. S. Millett, D. C. Shungu, *Biophys. J.* **53**, 145 (1988).
18. M. C. Bano, L. Braco, C. Abad, *FEBS Lett.* **250**, 67 (1989).
19. The gramicidin dimerization constant in ethanol is ~30 μM (*4*), and ~0.1% of the total gramicidin in the (14 nM) stock solution is intertwined dimers. This amount is in principle enough to account for all of the channel activity seen here.
20. D. W. Urry, M. M. Long, M. Jacobs, R. D. Harris, *Ann. N.Y. Acad. Sci.* **263**, 203 (1975).
21. I. Amdur and G. G. Hammes, *Chemical Kinetics: Principles and Selected Topics* (McGraw-Hill, New York, 1965), pp. 16–19.
22. We distinguish between slow permeation of gramicidin (monomers) across the bilayer, as evidenced by the maintained asymmetry in monolayer composition, and transfer of gramicidin at the start of the experiment, which constitutes a separate and transient process.
23. D. B. Sawyer, R. E. Koeppe II, O. S. Andersen, *Biophys. J.* **57**, 515 (1990).
24. J. T. Durkin, O. S. Andersen, F. Heitz, Y. Trudelle, R. E. Koeppe II, *Biophys. J.* **51**, 451a (1987).
25. Intertwined dimers of gA are left-handed helices (*6*), while the channel-forming $\beta^{6.3}$-helical dimers are right-handed helices [A. S. Arseniev, I. L. Barsukov, V. F. Bystrov, A. L. Lomize, Y. A. Ovchinnikov, *FEBS Lett.* **186**, 168 (1985); L. Nicholson and T. A. Cross, *Biochemistry* **28**, 9379 (1989); O. S. Andersen *et al.*, *Biophys. J* **57**, 100a (1990)].
26. The relative position of Trp in hydrophobicity scales varies with the methods used to establish the scales [D. M. Engelman, T. A. Steitz, A. Goldman, *Annu. Rev. Biophys. Chem.* **15**, 321 (1986)]. Methods that rely on the partitioning of Trp between water and nonpolar solvents (such as ethanol or octanol) tend to categorize Trp as quite hydrophobic, but these solvents have hydrogen-bond accepting groups. Methods that rely on the statistical distribution of residues in proteins of known structure or vapor-phase distribution tend to categorize Trp as only modestly hydrophobic. We also note that Trp has a high affinity for the membrane-solution interface [R. E. Jacobs and S. H. White, *Biochemistry* **28**, 3421 (1989)].
27. J.-L. Mazet, O. S. Andersen, R. E. Koeppe II, *Biophys. J.* **45**, 263 (1984).
28. H. Michel and J. Deisenhofer, *Curr. Top. Membr. Transp.* **36**, 53 (1990).
29. V. R. Lingappa, *J. Clin. Invest.* **83**, 739 (1989).
30. J. Kyte and R. F. Doolittle, *J. Mol. Biol.* **157**, 105 (1979).
31. Supported in part by NIH grants GM21342 and GM34968. We thank M. B. Becker, P. Daumas, J. T. Durkin, L. L. Providence, and D. B. Sawyer for helpful discussions and comments on the manuscript. A preliminary report has appeared [A. K. Maddock, R. E. Koeppe II, O. S. Andersen, *ICSU Short Rep.* **9**, 24 (1989)].

8 May 1990; accepted 30 July 1990

Binding of the Wilms' Tumor Locus Zinc Finger Protein to the EGR-1 Consensus Sequence

FRANK J. RAUSCHER III,* JENNIFER F. MORRIS, OLIVIA E. TOURNAY, DONNA M. COOK, TOM CURRAN

The Wilms' tumor locus (WTL) at 11p13 contains a gene that encodes a zinc finger–containing protein that has characteristics of a DNA-binding protein. However, binding of this protein to DNA in a sequence-specific manner has not been demonstrated. A synthetic gene was constructed that contained the zinc finger region, and the protein was expressed in *Escherichia coli*. The recombinant protein was used to identify a specific DNA binding site from a pool of degenerate oligonucleotides. The binding sites obtained were similar to the sequence recognized by the early growth response–1 (EGR-1) gene product, a zinc finger–containing protein that is induced by mitogenic stimuli. A mutation in the zinc finger region of the protein originally identified in a Wilms' tumor patient abolished its DNA-binding activity. These results suggest that the WTL protein may act at the DNA binding site of a growth factor–inducible gene and that loss of DNA-binding activity contributes to the tumorigenic process.

WILMS' TUMOR (WT) IS A MALIGNANCY of the kidney that occurs in children and is associated with aniridia, mental retardation, and urogenital malfunctions (the WAGR syndrome) (*1–3*). As with retinoblastoma, both hereditary and sporadic forms of WT have been described (*4*). Several cytogenetic studies have linked a specific chromosomal abnormality at the 11p13 locus to the heritable form of the tumor (*2, 3*). Furthermore, loss of heterozygosity at polymorphic loci that surround 11p13 has been observed in sporadic WT (*5*). Introduction of a normal human chromosome 11 into a WT cell line suppresses some aspects of the malignant phenotype (*6*), further suggesting that a tumor suppressor gene on chromosome 11 is involved in the genesis of WT.

Candidate complementary DNAs (cDNAs) for the WT gene have been isolated (*7, 8*). One was obtained with a long-range restriction map of the WAGR region, which allowed localization of the WT gene to a 345-kilobase region of chromosome 11 (*9*); a cDNA clone was subsequently isolated from this region (*7*). In another approach, the presence of CpG islands adjacent to the WT locus (WTL) was exploited in conjunction with chromosome jumping to isolate a similar cDNA (*8*). The gene is expressed in high amounts in embryonic kidney and adult spleen (*7, 8*).

The predicted protein product of the WTL contains a region rich in glutamine and proline residues, and four contiguous zinc fingers of the Cys_2-His_2 class (*7, 8*). The presence of these two structural motifs implies that the WTL protein is a sequence-specific nucleic acid–binding protein that may function as a transcriptional regulator (*10*). In this report, we have initiated a biochemical characterization of the WTL protein by identifying a DNA target sequence that is recognized by the WTL protein.

Our strategy was to express the zinc finger domain of the WTL protein in *E. coli* and to use this protein as an affinity matrix for isolation of a DNA target sequence. The zinc finger region (termed WT-ZF) was reconstructed from synthetic oligonucleotides with the use of an overlapping PCR strategy for gene synthesis (Fig. 1A) (*11*). Six histidine residues were added to the NH_2-terminus to facilitate purification of the protein with a nickel-chelate affinity resin (*11, 12*). The purified WT-ZF protein migrated with an apparent molecular size of 21,500 kilodaltons (kD) on SDS-polyacrylamide gels (Fig. 1B, lane 2).

A modification of the method developed by Struhl and colleagues (*13*) was used to isolate DNA sequences that were recognized specifically by WT-ZF (Fig. 2A). A degenerate oligonucleotide that contained random nucleotides at 25 consecutive positions flanked by Xho I and Eco RI sites was synthesized. By self-annealing this oligonucleotide and extending with DNA polymerase in the presence of deoxynucleotide triphosphates (dNTP's), a completely degenerate library of double-stranded oligonucleotides was obtained. A probe was prepared with ^{32}P-labeled dNTP's that allowed verification of the presence of potential binding sites (Fig. 2A). The probe was then selected

F. J. Rauscher III, J. F. Morris, O. E. Tournay, D. M. Cook, The Wistar Institute, 3601 Spruce Street, Philadelphia, PA 19104.
T. Curran, Roche Institute of Molecular Biology, Department of Molecular Oncology and Virology, Roche Research Center, Nutley, NJ 07110.

*To whom correspondence should be addressed.